THE JOURNAL OF BIOLOGICAL CHEMISTRY VOL. 285, NO. 7, pp. 4298–4306, February 12, 2010


# Cdc42p Is Activated during Vacuole Membrane Fusion in a Sterol-dependent Subreaction of Priming*

Received for publication, October 9, 2009, and in revised form, November 29, 2009 Published, JBC Papers in Press, December 10, 2009, DOI 10.1074/jbc.M109.074609

**Lynden Jones, Kelly Tedrick, Alicia Baier, Michael R. Logan, and Gary Eitzen**[1]

*From the Department of Cell Biology, University of Alberta, Edmonton, Alberta T6G 2H7, Canada*

**Cdc42p is a Rho GTPase that initiates signaling cascades at spatially defined intracellular sites for many cellular functions. We have previously shown that Cdc42p is localized to the yeast vacuole where it initiates actin polymerization during membrane fusion. Here we examine the activation cycle of Cdc42p during vacuole membrane fusion. Expression of either GTP- or GDP-locked Cdc42p mutants caused several morphological defects including enlarged cells and fragmented vacuoles. Stimulation of multiple rounds of fusion enhanced vacuole fragmentation, suggesting that cycles of Cdc42p activation, involving rounds of GTP binding and hydrolysis, are required to propagate Cdc42p signaling. We developed an assay to directly examine Cdc42p activation based on affinity to a probe derived from the p21-activated kinase effector, Ste20p. Cdc42p was rapidly activated during vacuole membrane fusion, which kinetically coincided with priming subreaction. During priming, Sec18p ATPase activity dissociates SNARE complexes and releases Sec17p, however, priming inhibitors such as Sec17p and Sec18p ligands did not block Cdc42p activation. Therefore, Cdc42p activation seems to be a parallel subreaction of priming, distinct from Sec18p activity. Specific mutants in the ergosterol synthesis pathway block both Sec17p release and Cdc42p activation. Taken together, our results define a novel sterol-dependent subreaction of vacuole priming that activates cycles of Cdc42p activity to facilitate membrane fusion.**

Cdc42p is a member of the Ras homology (Rho)[2] family of small monomeric GTPases. These small GTPases regulate many cellular mechanisms including polarized membrane traffic, cell adhesion, cell motility, gene expression, and other morphogenic processes (1–3). The activity of Cdc42p is regulated by cycling between GDP-bound inactive and GTP-bound active states. Extensive structural studies have shown that large conformational changes occur between the two states in two regions designated switch I and switch II. These switch regions play an important role in interactions with downstream targets to transduce upstream signals. The GTP/GDP cycle is regulated by three accessory factors: GAPs (GTPase-activating proteins), GEFs (guanine nucleotide exchange factors), and GDI (GDP dissociation inhibitor). GAPs accelerate the intrinsic GTPase activity resulting in the inactive GDP-bound form, whereas GEFs facilitate the exchange of GDP for GTP resulting in the active GTP-bound form. Specific knowledge of this regulatory mechanism has made it possible to prepare mutant Rho GTPase that are constitutively active by inhibiting their ability to hydrolyze GTP, or constitutively inactive by inhibiting their ability to exchange GDP for GTP (1). GDI not only blocks the activation cycle, but can also extract GTPases from membranes, which allows for new membrane delivery from a soluble pool.

There is a significant body of evidence describing how Cdc42p controls actin filament (F-actin) remodeling for cell movement; however, much less is known about how Cdc42p controls intracellular membrane traffic (2). Current literature suggests that Rho GTPases regulate two subreactions. First, they induce the formation of cytoskeletal tracks that are needed for transport of vesicles prior to exocytosis (3). A second role for actin remodeling in membrane fusion is not associated with transport. We have shown that actin disassembly is an early subreaction of vacuole membrane fusion, whereas the formation of F-actin is needed for fusion and is likely catalyzed by components activated by Cdc42p at the membrane surface (4, 5). Recently, Cdc42p signaling was shown to facilitate exocytosis in PC12 cells by promoting actin polymerization through WASP (6), and we have shown that verprolin, the binding partner of WASP, plays a role in vacuole fusion (7). Therefore, it is likely that multiple vesicle transport and fusion processes include a Cdc42p-regulated actin remodeling subreaction.

Numerous subcellular localizations have been shown for Cdc42p. Cdc42p is primarily localized to the bud tip in yeast where it initiates polarity via spatially directed vesicular transport (8). In addition to initiating polarity, Cdc42p also regulates membrane docking and fusion at the plasma membrane. We have recently shown that Cdc42p is localized to the yeast vacuole where it controls actin polymerization activity during homotypic vacuole fusion (5). However, mechanisms that trigger the activation of Cdc42p at these sites are unknown.

Here we report the morphological effects of expressing Cdc42p mutants that are locked in specific nucleotide conformations. Overexpression of either constitutively active or dominant-negative Cdc42p resulted in vacuole fragmentation. A single fusion stimulus was able to trigger vacuole membrane fusion except when dominant-negative Cdc42p was expressed;

* This work was supported by a grant from the Canadian Institutes of Health Research (CIHR).

[1] To whom correspondence should be addressed: 5-14 Medical Science Bldg., University of Alberta, Edmonton, AB T6G 2H7, Canada. Tel.: 780-492-6062; Fax: 780-492-0450; E-mail: gary.eitzen@ualberta.ca.

[2] The abbreviations used are: Rho, Ras homology; ATPreg, ATP-regenerating system; F.R.B., fusion reaction buffer; GST, glutathione *S*-transferase protein; GST-CBD, GST-tagged probes derived from the Cdc42p/Rac binding domains of p21-activated kinase; HA, hemagglutinin antigen; kan, kanamycin; GAP, GTPase-activating protein; GEF, guanine nucleotide exchange factors; GDI, GDP dissociation inhibitor; GTPγS, guanosine 5′-3-*O*-(thio)triphosphate; PIPES, 1,4-piperazinediethanesulfonic acid; WT, wild type; PIC, protease inhibitor mixture; ALP, alkaline phosphatase.

**TABLE 1**
***Saccharomyces cerevisiae* strains used in this study**

| Strain | Genotype | Source |
|---|---|---|
| BJ5459 | *MatA, pep4::HIS3, prb1-Δ1.6R, his3, leu2, ura3, lys2, trp1, can1* | [a] |
| DKY6281 | *MatA, pho8::TRP1, his3, leu2, ura3, lys2, suc2* | 11 |
| K91–1A | *MatA, pho8::AL134, pho13::pPH13, his3, ura3, lys2* | 11 |
| DJTD2-16A | *MatA, his4, leu2, ura3, trp1, cdc42-1* | [a] |
| TD4 | *MatA, his4, leu2, ura3, trp1* | 22 |
| BY4742 | *Matα, his3, leu2, ura3, lys2* | [b] |
| *erg2Δ* | *Matα, his3, leu2, ura3, lys2, erg2::kanMX* | [b] |
| *erg3Δ* | *Matα, his3, leu2, ura3, lys2, erg3::kanMX* | [b] |
| *erg4Δ* | *Matα, his3, leu2, ura3, lys2, erg4::kanMX* | [b] |
| *erg5Δ* | *Matα, his3, leu2, ura3, lys2, erg5::kanMX* | [b] |
| *erg6Δ* | *Matα, his3, leu2, ura3, lys2, erg6::kanMX* | [b] |

[a] ATCC.
[b] Open Biosystems.

however, multiple rounds of fusion required cycles of Cdc42p activation. We also provide a method for the analysis of *Saccharomyces cerevisiae* Cdc42p activation on purified vacuole membranes. The activation mechanism showed temporal regulation and required ergosterol that is needed during vacuole priming subreactions. Our results define the cyclical activation of Cdc42p as a subreaction of the vacuole membrane fusion mechanism.

## EXPERIMENTAL PROCEDURES

*Yeast Strains and Growth*—Yeast strains used in this study are listed in Table 1. Cdc42p wild-type and mutant overexpression strains were prepared using Drop&Drag cloning (9) as previously described (5). Briefly, the *CDC42* open reading frame was cloned into pBluescript SK II(−) (Stratagene) from genomic DNA using orf primers: 5′Cdc42p cggatcccaaacgctaaagtgtg; 3′Cdc42p, cgggatccatgggcatatactaatatga. Selected amino acid changes were made using QuikChange II site-directed mutagenesis (Stratagene) and confirmed by sequence analysis (5). Constructs were amplified from plasmids using rec1/rec2 primers (9), transformed into yeast strains in the presence of SalI cut pGREG535 and grown on CSM-leu agar plates. Strains were normally grown in YPD (1% yeast extract, 2% peptone, 2% dextrose). Plasmid-bearing strains were grown in YPDG-kan (1% yeast extract, 2% peptone, 1% dextrose, 1% galactose, 50 μg/ml kanamycin), which results in mutant Rho protein overexpression from the galactose inducible *GAL1* promoter.

*Protein Preparation*—The Ste20p-derived Cdc42p activation probe (GST-CBD) was prepared by cloning a PCR fragment *STE20*, encoding amino acids 331–410, into pGEX-4TI. The primers used were 5′Ste20-CBD cgggatccataaccaccgctttgaggat, and 3′Ste20-CBD cggaattcttagttgaaagtcttgaacattt. Fusion proteins were expressed in *Escherichia coli* BL21. The GST-CBD affinity probe was prepared and used as previously described (10). Yeast cytosol was prepared from strain K91-1A grown to an $A_{600} \sim 4$, by vortexing cells for 10 min at 4 °C with glass beads using a ratio of 1 volume of glass beads to 2 volumes of cells, resuspended at 1/100th the original culture volume in lysis buffer (20 mM PIPES-KOH, pH 6.8, 200 mM sorbitol, 1 mM Mg-ATP, 1 mM dithiothreitol, 2× PIC). PIC was made as a 60× stock solution (60× PIC = 12 μg/ml leupeptin, 24 μg/ml pepstatin, 25 mM *o*-phenanthroline, 6 mM Pefabloc SC). Lysates were cleared by centrifugation at 25,000 × *g* for 30 min at 4 °C.

*Cdc42p Activation Assays*—Activated (GTP-bound) vacuolar or cytosolic Cdc42p was determined by affinity binding and pull-down with glutathione-Sepharose bound Cdc42p activation probes, GST-CBD. Specific nucleotide-bound states of lysate or vacuolar GTPases were prepared by chemical nucleotide exchange, which involved incubation for 5 min at 30 °C in the presence of 3 mM EDTA and 40 μM nucleotide (GDP, GTP, or GTPγS for chemical pre-activation) which facilitates nucleotide exchange. The exchange reaction was quenched by addition of 10 mM $MgCl_2$, which effectively locks GTPases in specific nucleotide-bound states (10). To assay Cdc42p activation, 200 μg of lysate or 50 μg of vacuoles and 30 μg of immobilized GST-CBD were incubated in a volume of 400 μl H-buffer (20 mM HEPES-KOH, pH 7.5, 1 mM dithiothreitol, 3 mM $MgCl_2$, 60 mM NaCl, 0.5% Nonidet P-40), for 30 min at 4 °C. The bead pellet was washed four times with H-buffer and resuspended in 50 μl of Laemmli sample buffer. Half the sample was analyzed by SDS-PAGE and immunoblot using anti-Cdc42p (y-191, Santa Cruz Biotechnology). Immunoblots were detected and quantified using IR-Dye800 fluorescently tagged secondary antibodies (Rockland Immunochemicals) and an Odyssey image analysis system (LiCor).

*Vacuole Isolation, Fusion, Sec17p Release, and GTPase Activation Reactions*—Vacuoles were isolated from yeast spheroplasts by flotation on Ficoll gradients. *In vitro* membrane fusion reactions were performed as previously described (11). Standard fusion reactions contained 3.5 μg of vacuoles from each of BJ5459 (pro-ALP fusion reporter) and DKY6251 (protease donor to cleave pro-ALP upon fusion) in 30 μl of fusion reaction buffer (F.R.B. = 20 mM PIPES-KOH, pH 6.8, 125 mM KCl, 5 mM $MgCl_2$, 200 mM sorbitol, 10 μM CoA, 1× PIC), 1× ATPreg (1× ATP-regenerating system: 0.5 mM ATP, 0.5 mM $MgCl_2$, 25 mM creatine phosphate, 0.25 mg/ml creatine kinase), and 0.5 mg/ml cytosol. To assay for Sec17p release, standard fusion reactions were incubated without cytosol, but in the presence of 5 μg/ml Sec18p and 10 μg/ml IB2. Vacuole-free supernatants were prepared by centrifugation at 18,000 × *g* for 5 min and then analyzed by immunoblot using an Odyssey imaging system. To assay Cdc42p activation, standard reactions contained 50-μg vacuoles in 200 μl that were preincubated at 27 °C in F.R.B., 1× ATPreg, 0.5 mg/ml cytosol, and 40 μM GTPγS to facilitate the detection of activation. Unless indicated (*i.e.* Fig. 6*C*), vacuoles were re-isolated (centrifugation at 18,000 × *g*, 4 °C, 5 min) from reactions after 2-fold dilution in cold PS buffer and then probed for activated Cdc42p.

*Microscopy and Cellular Analyses*—Vacuoles were stained by incubating live cells with 3 μM FM4-64 (Invitrogen) for 20 min followed by a 2-h chase in dye-free medium. Vacuole morphology was initially observed while cells were in YPDG-kan medium ($A_{600} \sim 1$), or after sequential incubation for <5 min in hypotonic conditions (10-fold dilution in water), hypertonic conditions (NaCl added to 0.4 M), and again in hypotonic conditions. Hypotonic stress has previously been shown to induce vacuole fusion *in vivo* (12), whereas hypertonic stress has been shown to induce vacuole fission *in vivo* (13). Images were acquired using an Axioskop2 with a 100×/1.4 NA plan apochromat oil immersion len (Zeiss), a CoolSnap HQ camera (Photometrics) and ImagePro Plus software (Media Cybernetics).

Relative cell size was analyzed by flow cytometry forward scatter and quantitatively measured from bright field images of unbudded cells using ImageJ.

## RESULTS

*Effect of Cdc42p Mutant Allele Expression on Vacuole Morphology*—Cdc42p is a Rho GTPase, which acts as molecular switch that is activated by GTP binding. We have previously shown that Cdc42p localizes to the vacuole and regulates membrane-associated actin polymerization during membrane fusion (5). To further characterize the role of Cdc42p in determining vacuole fusion competency we prepared several strains that overexpress mutant alleles with fixed "nucleotide-locked" states. We cloned a constitutively active mutant, Cdc42p-G12V, blocked in GTP hydrolysis, which remains GTP-bound, and a dominant-negative mutant, Cdc42p-T17N, blocked in GDP/GTP exchange, which remains GDP-bound (14, 15). Expression levels were similar when analyzed by immunoblot (Fig. 1*A*), and mutant specificity was confirmed by a Cdc42p activation assay which is subsequently described (*see* Fig. 5*B*). Growth assays showed that all strains were viable when grown at 27 °C (Fig. 1*B*). Wild-type Cdc42p overexpression rescued growth of the *cdc42-1* mutant strain at its non-permissive temperature (37 °C) whereas "nucleotide-locked" *CDC42* mutant alleles did not (Fig. 1*B*). These growth assays demonstrate that expression of mutant alleles is not toxic under standard growth conditions, but do not rescue growth defects in the absence of Cdc42p. Mutant allele expression also affected cell size, as shown qualitatively by increased forward-scatter when analyzed by flow cytometry (Fig. 1*C*). Quantitative measurements from microscopic images showed a 31, 42, and 55% increase in size due to overexpression of WT, constitutively active, and dominant-negative alleles, respectively, compared with empty vector transformants (Fig. 1*D*).

We next examined the effects of *CDC42* wild-type and mutant alleles on vacuole morphology. We have previously used vacuole fragmentation (*i.e.* increased vacuole lobe numbers) as an indicator of membrane fusion defect (16). When *CDC42* mutant allele expression was not induced, all strains were indistinguishable from wild-type and displayed the normal phenotype of a few round vacuoles per cell (data not shown). Overexpression of wild-type *CDC42* resulted in slightly increased vacuole fragmentation (Fig. 2*e*). Interestingly, overexpression of either constitutively-active or dominant-negative *CDC42* resulted in enlarged cells with highly fragmented vacuoles (Fig. 2, *i* and *m*, respectively). The effect on vacuole morphology was quantified by categorizing cells according to the number of vacuole lobes. This analysis confirmed that expression of either *CDC42* mutant allele resulted in increased vacuole fragmentation with the dominant-negative allele having the greatest effect (Fig. 3, *panel A*).

To verify that vacuole fragmentation was the result of a membrane fusion defect, we exposed cells to hypotonic stress which has previously been shown to trigger rapid vacuole fusion (12). Most strains showed a normal response and went from having multiple vacuoles to one vacuole per cell (Fig. 2, compare *Normal versus Hypotonic 1 columns*). However, overexpression of the Cdc42p-T17N dominant-negative allele

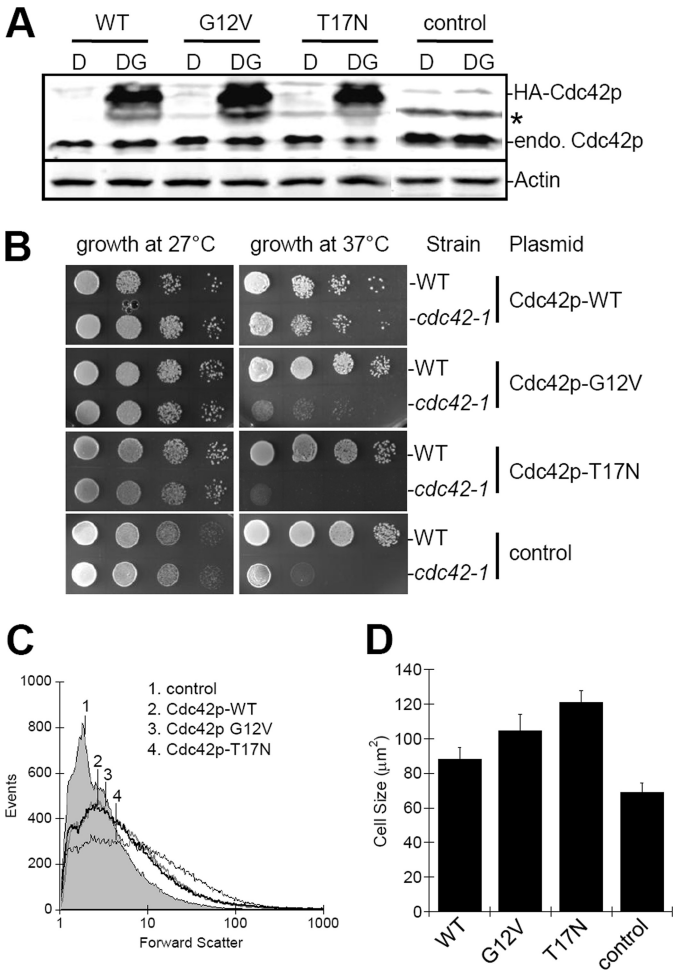


FIGURE 1. **Overexpression of HA-tagged Cdc42p.** *A*, yeast strain BY4742 was transformed with plasmid pGREG-535 ($P_{GAL1}$-7HA overexpression vector) containing WT, constitutively active (*G12V*), or dominant-negative (*T17N*) alleles of *CDC42*. Transformants were grown in YPD-kan (*D*) or YPDG-kan (*DG*), which contains 1% galactose to induce expression of cloned alleles. For *control*, BY4742 was transformed with empty vector and grown in YPD or YPDG. Equal amounts of lysate were analyzed. * indicates a background band. *B*, viability assay of strains overexpressing Cdc42p WT and mutant clones. Note that growth of the parental strain, TD4, is not affected whereas growth of the *cdc42-1* temperature-sensitive strain, DJTD2-16A, is only rescued by expression of Cdc42p-WT. *C*, relative size of cells from strains in *A*, as determined by flow cytometry forward scatter measurements of 50,000 cells. *Numbered lines* indicate the mean for each sample. *D*, cell size quantitatively determined by cross-sectional area measurements of bright-field images imported into ImageJ (±S.E., $n = 20$ cells).

blocked vacuole fusion triggered by hypotonic stress (Fig. 2*n*) confirming the need for Cdc42p activation for fusion. Quantification of vacuole fragmentation confirmed that dominant-negative Cdc42p-T17N showed a 50% increase in vacuole fragmentation (Fig. 3, *panel B*). Hypertonic stress triggers vacuole fragmentation (13) and can be used to examine whether mutants affect vacuole fission. Stress-induced fragmentation was normal in all strains (Fig. 2, *Hypertonic column* and Fig. 3, *panel C*).

The accumulation of fragmented vacuoles during normal growth suggests that Cdc42p cycling may be needed for fusion. However, an initial hypotonic stimulus triggered fusion in all cases except when dominant-negative Cdc42p-T17N was expressed. This result is consistent with an initial round of fusion requiring only activated Cdc42p, while multiple rounds

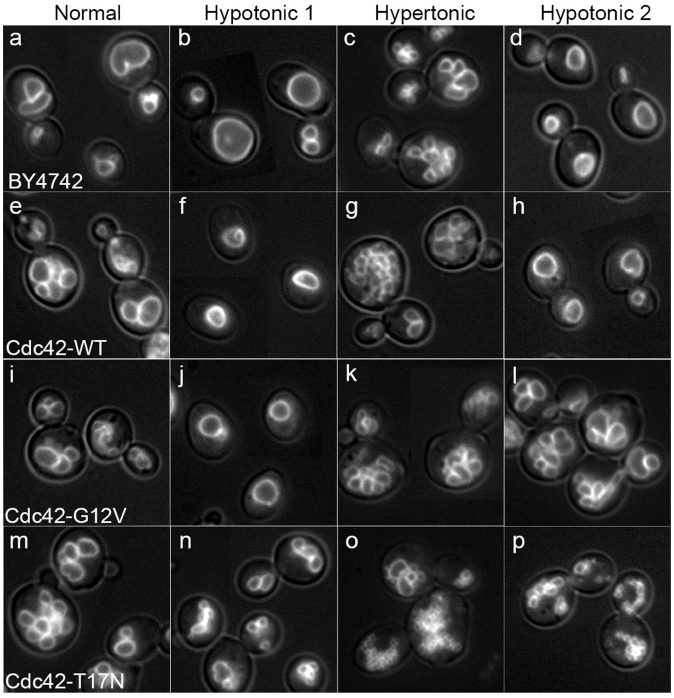


FIGURE 2. **Characterization of vacuole morphology in *CDC42* mutant strains.** Strain BY4742 was transformed with the empty vector pGREG535 (*BY4742*), or with vectors that overexpress wild type (*Cdc42p-WT*), constitutively active (*Cdc42p-G12V*), or dominant-negative (*Cdc42p-T17N*) Cdc42p from the *GAL1* galactose-inducible promoter. Cells were grown in YPDG-kan to ~0.6 $A_{600}$, vacuoles were stained with FM4-64, and cells were visualized by fluorescence microscopy (*Normal*). Vacuolar hypotonic and hypertonic stress response was examined by dilution in water (*Hypotonic 1*) or incubation in 0.4 M NaCl, (*Hypertonic*). Multiple rounds of vacuole fusion were examined after sequential hypotonic-hypertonic and hypotonic stresses (*Hypotonic 2*). Panels are 30 $\mu$m × 30 $\mu$m.

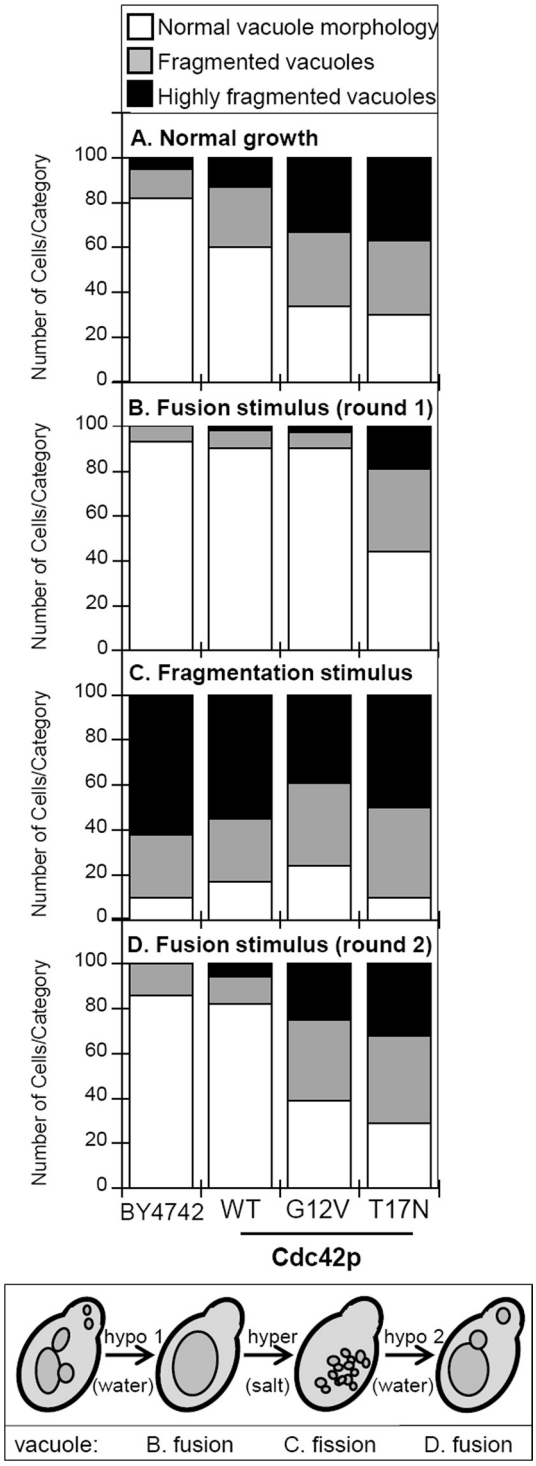


FIGURE 3. **Quantification of vacuole fragmentation levels in strains expressing *CDC42* mutant alleles.** 100 cells for each strain depicted in Fig. 2 were categorized as having normal vacuole morphology (<4 vacuole lobes), fragmented vacuoles (4–10 vacuole lobes) or highly fragmented vacuoles (>10 vacuole lobes). Vacuole morphology was quantified in strains grown in YPDG-kan (*A*), after hypotonic stress via dilution in water (*B*), after hypertonic stress via addition of NaCl to 0.4 M (*C*), or after a second hypotonic stress treatment (*D*). The treatment scheme is shown in the *lower box* with the intended result on vacuole morphology indicated.

of fusion might require complete cycling. To examine multiple rounds of fusion we exposed cells to a sequential series of hypotonic-hypertonic-hypotonic stresses (Fig. 2, *Hypotonic 2 column*). This treatment resulted in the appearance of fragmented vacuoles in strains expressing constitutively-active Cdc42p-G12V (Fig. 2*l*); quantification revealed a 45% increase in vacuole fragmentation compared with a single fusion stimulus (Fig. 3, compare *G12V* in *panels B* and *D*). Strains expressing dominant-negative Cdc42p-T17N showed an augmented fusion defects after the second round of fusion stimulus (Figs. 2*p* and 3*D*). Taken together, these data are consistent with the need for complete cycles of Cdc42p activation for vacuole fusion.

*Effect of Cdc42p Mutant Allele Expression on in Vitro Vacuole Fusion*—We next examined the influence of mutant Cdc42p proteins on membrane fusion using a well characterized *in vitro* vacuole fusion assay (17). For this assay, vacuoles are purified from two strains; one strain has vacuolar luminal proteases, but is deleted for the gene encoding ALP; the other strain lacks proteases and therefore accumulates catalytically inactive pro-ALP. Equal concentrations of these vacuoles are mix and incubated with ATP, salts and cytosol. Vacuole-to-vacuole membrane fusion enables content mixing, allowing protease to gain access to pro-ALP converting it to the active form. Therefore, the levels of active ALP are proportional to fusion.

The fusion of vacuoles purified from strains expressing "nucleotide-locked" Cdc42p mutants was compared with strains expressing wild-type Cdc42p. Vacuoles purified from strains expressing constitutively active Cdc42p-G12V showed kinetically enhanced fusion rates at early time points; however

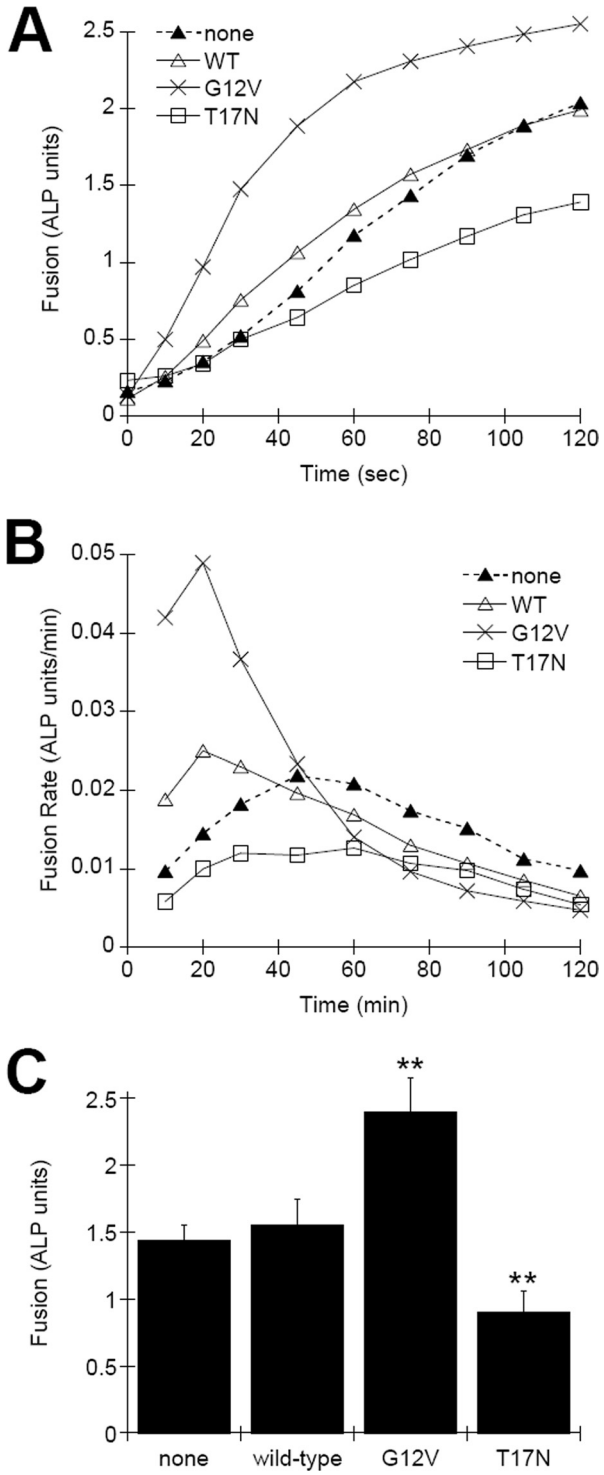


FIGURE 4. **Effect of Cdc42p mutant protein expression on *in vitro* vacuole fusion.** *A*, fusion of vacuoles isolated from BJ5459 and DKY6281 strains expressing wild-type Cdc42p-WT, constitutively active Cdc42p-G12V, or dominant-negative Cdc42p-T17N. At the indicated times, reactions were stopped by placing on ice and assayed for fusion signal via ALP enzyme assay. Shown are the average signals from two independent experiments. *B*, rate of fusion determined by integration of fusion curves in *A*. *C*, statistical analysis of fusion signals obtained after 1 h of incubation (± S.E., $n = 4$, **, $p < 0.001$).

this was not sustained throughout the reaction (Fig. 4, *A* and *B*). Cdc42p-T17N expression reduced fusion kinetics. These results implicate the need for Cdc42p activation during the initial priming stage of vacuole fusion. Statistical analysis of standard fusion reactions incubated for 1 h showed that Cdc42p-G12V increased vacuole fusion signals by an average of 66%, whereas Cdc42p-T17N reduced fusion by 57% (Fig. 4*C*).

*Detection of Cdc42p Activation*—To directly examine Cdc42p signaling on the vacuole membrane, we developed an assay to detect Cdc42p activation during *in vitro* fusion reactions. A previously developed Cdc42p activation assays used affinity to a GST-tagged probes derived from the Cdc42p binding domains (CBD) of p21-activated kinase 1 (GST-CBD), a downstream effector protein of Cdc42/Rac (10). We constructed a similar probe from the CBD domain of p21-activate kinase, Ste20p (Fig. 5*A*; amino acids 211–334; Ref. 18). Lysates were prepared from strains overexpressing mutant and wild-type Cdc42p. This probe showed high levels of association with constitutively active Cdc42p-G12V, which is in the GTP-bound state, and very little association with dominant-negative Cdc42p-T17N, which is in the GDP-bound state (Fig. 5*B*).

We next tested whether the Cdc42p activation probe would specifically detect endogenous activated Cdc42p. Yeast vacuoles were purified and subjected to a chemical nucleotide exchange protocol (10) to obtain specific nucleotide-bound states, and then incubated with GST-CBD. Preincubation with GDP resulted in no association with the activation probe; however high levels of binding were observed when GTPγS was exchanged, and somewhat less when GTP was exchanged (Fig. 5*C*). These results show that GST-CBD specifically detected GTP-bound Cdc42p on the vacuole membrane. The endogenous GTPase activity of Cdc42p in our samples seemed to be sufficiently high to quickly hydrolyze GTP during incubations. Therefore, very little association was detected unless non-hydrolyzable GTPγS was included in reactions. Spontaneous binding of GTPγS did not occur since incubation on ice resulted in no detectable Cdc42p association with the probe in all experiments.

*Cdc42p Activation during Membrane Fusion*—Because our primary interest is the regulation of membrane fusion, we next examined whether Cdc42p could be activated by incubations that stimulate vacuole fusion. Very low levels of activated Cdc42p were detectable when vacuoles were preincubated in membrane fusion reaction buffer (Fig. 5*D*, *left panel*). Activated levels were significantly enhanced when GTPγS was included in the reaction buffer, to levels comparable to chemical nucleotide exchange (Fig. 5*D*, *right panel*). This indicates that Cdc42p undergoes activation during vacuole fusion, but also quickly hydrolyzes bound nucleotide. To avoid underestimation of activation levels due to GTP hydrolysis, GTPγS was included in all activation assays.

We next assayed the kinetics of Cdc42p activation during vacuole fusion. Vacuoles were incubated in fusion reaction buffer and at specific times aliquots were removed and assayed for membrane fusion via content mixing assay. Cdc42p activation via association with GST-CBD was examined in parallel reactions. Fusion signals increased linearly for 60 min; however, the kinetics of Cdc42p activation did not mirror the kinetics of fusion (Fig. 6*A*). Instead, Cdc42p was rapidly activated, reaching maximum levels by 20 min (Fig. 6, *A* and *B*). This would kinetically coincide with an early subreaction of membrane fusion such as priming (17). Sec17p is released from vacuoles

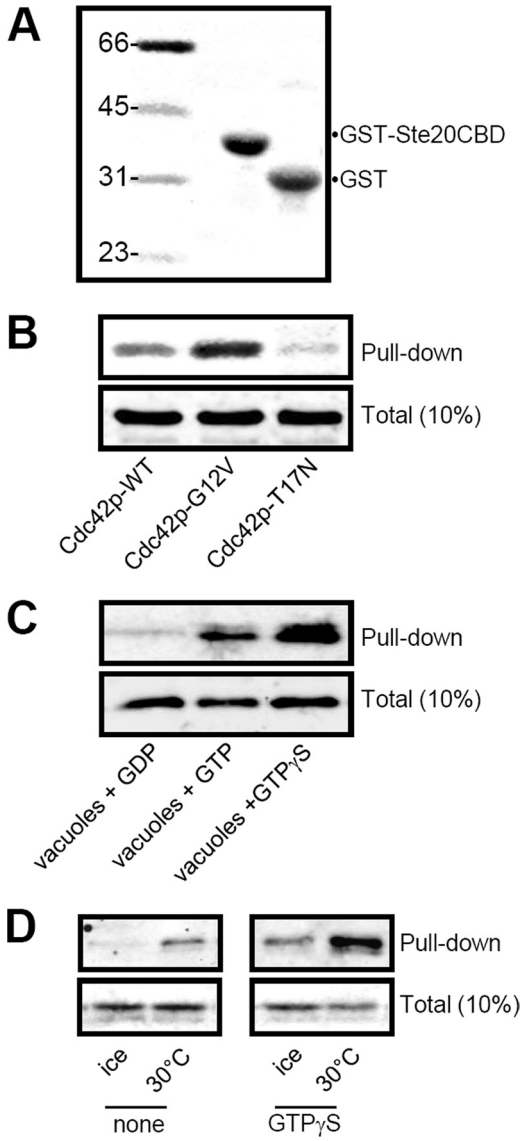


FIGURE 5. **Assay of Cdc42p activation in yeast.** The CBD of yeast Ste20p was cloned as GST fusion proteins and expressed in *E. coli*. *A*, 30 $\mu$g of GST-CBD probe or GST was immobilized on glutathione beads and 10% was analyzed by immunoblot. *B*, incubation of GST-CBD probe with 200 $\mu$g of yeast whole-cell lysate prepared from strain overexpressing Cdc42p-WT, Cdc42p-G12V (GTP-bound), or Cdc42p-T17N (GDP-bound). *C*, incubation of GST-CBD probe with 50 $\mu$g of purified vacuoles subjected to GDP, GTP, or GTP$\gamma$S nucleotide exchange as described under "Experimental Procedures." *D*, determination of Cdc42p activation during membrane fusion. 50 $\mu$g of purified vacuoles were incubated in 200 $\mu$l of F.R.B., ATPreg, and cytosol in the absence (none) or presence of 40 $\mu$M GTP$\gamma$S. All samples were incubated for 30 min on ice or at 30 °C, as indicated, and then 30 $\mu$g of GST-CBD beads were added to affinity isolate-activated (GTP-bound) Cdc42p (*Pull-down*). *10% Total* refers to Cdc42p load controls.

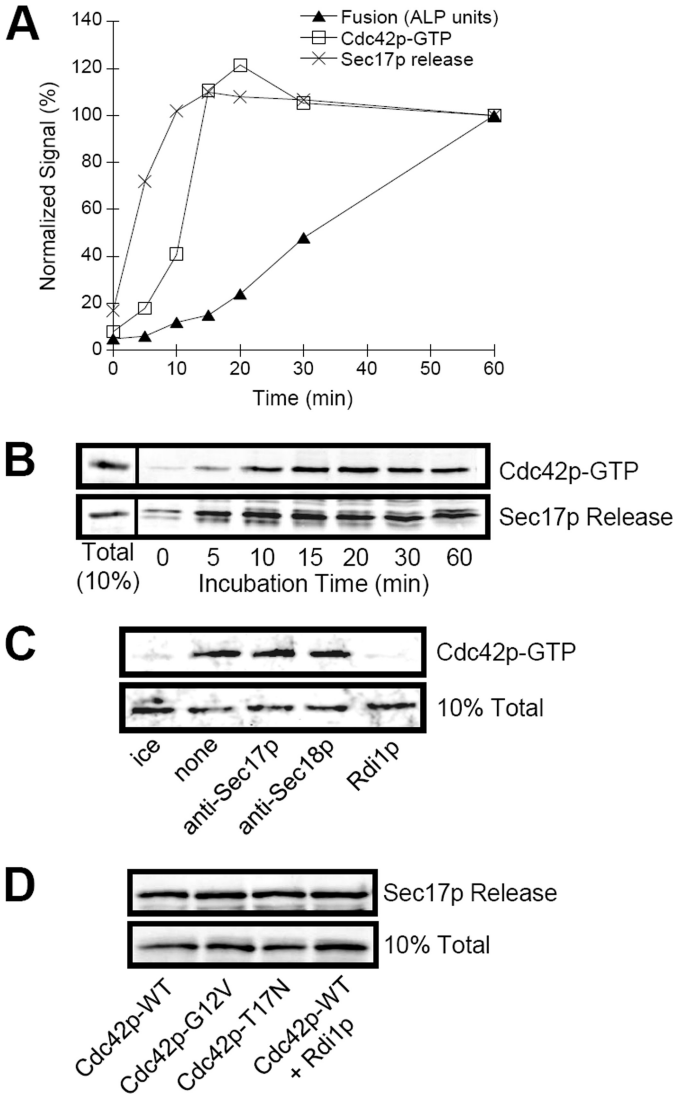


FIGURE 6. **Analysis of vacuole-priming subreactions.** Standard vacuole fusion reactions were performed to assay for levels of fusion and Cdc42p activation and Sec17p release as described under "Experimental Procedures." At the indicated times, reactions were stopped by placing on ice and assayed for fusion signal via ALP enzyme assay. Sec17p release and Cdc42p activation via pull-down with the GST-CBD probe were assayed in parallel reactions. *A*, quantification of fusion, Cdc42p activation, and Sec17p release, normalized to 60-min reactions. Shown are the average signals from at least three independent experiments. *B*, typical immunoblots showing the time course for Cdc42p activation and Sec17p release that were quantified by band densitometry. *C*, effect of incubation with priming inhibitors on Cdc42p activation. Reactions were incubated for 30 min at 30 °C (or on ice) in the presence of no inhibitor (*none* and *ice*), 150 $\mu$g/ml anti-Sec17p, anti-Sec18p antibodies (priming inhibitors), or Rdi1p (Rho GDP dissociation inhibitor). The *upper panel* shows the levels of Cdc42p-GTP via pull-down by GST-CBD probe that was added directly to reactions (*i.e.* without membrane reisolation due to potential Rdi1p extraction of Cdc42p). The *lower panel* shows 10% of the total Cdc42p in each reaction. *D*, effect of expressing Cdc42p mutant proteins, or incubation with 150 $\mu$g/ml Rdi1p, on Sec17p release. *10% Total* refers to load controls for Cdc42p (*A*, *upper panel*; *C*) and Sec17p (*A*, *lower panel*; *D*).

during priming and the kinetics of Sec17p release slightly preceded Cdc42p activation (Fig. 6, *A* and *B*), which suggests these reactions might occur sequentially during priming. Reactions that contained priming inhibitors such as Sec17p and Sec18p antibodies failed to block Cdc42p activation, whereas incubation on ice or with the activation inhibitor Rdi1p significantly blocked activation (Fig. 6*C*). Likewise, Sec17p release was not inhibited by expression of mutant Cdc42p or incubation with Rdi1p (Fig. 6*D*). These results suggest that Cdc42p activation occurs as parallel subreaction of priming, along with Sec18p-driven release of Sec17p.

*Sterol-dependence of Cdc42p Activation*—Ergosterol is required for Sec18p priming and facilitates vacuole fusion (7, 19). It has been shown to be one of the first lipid components organized into fusogenic domains of docked vacuoles (20). Vacuole fusion is inhibited in mutant strains that are defective in ergosterol synthesis. This can be observed by high levels of vac-

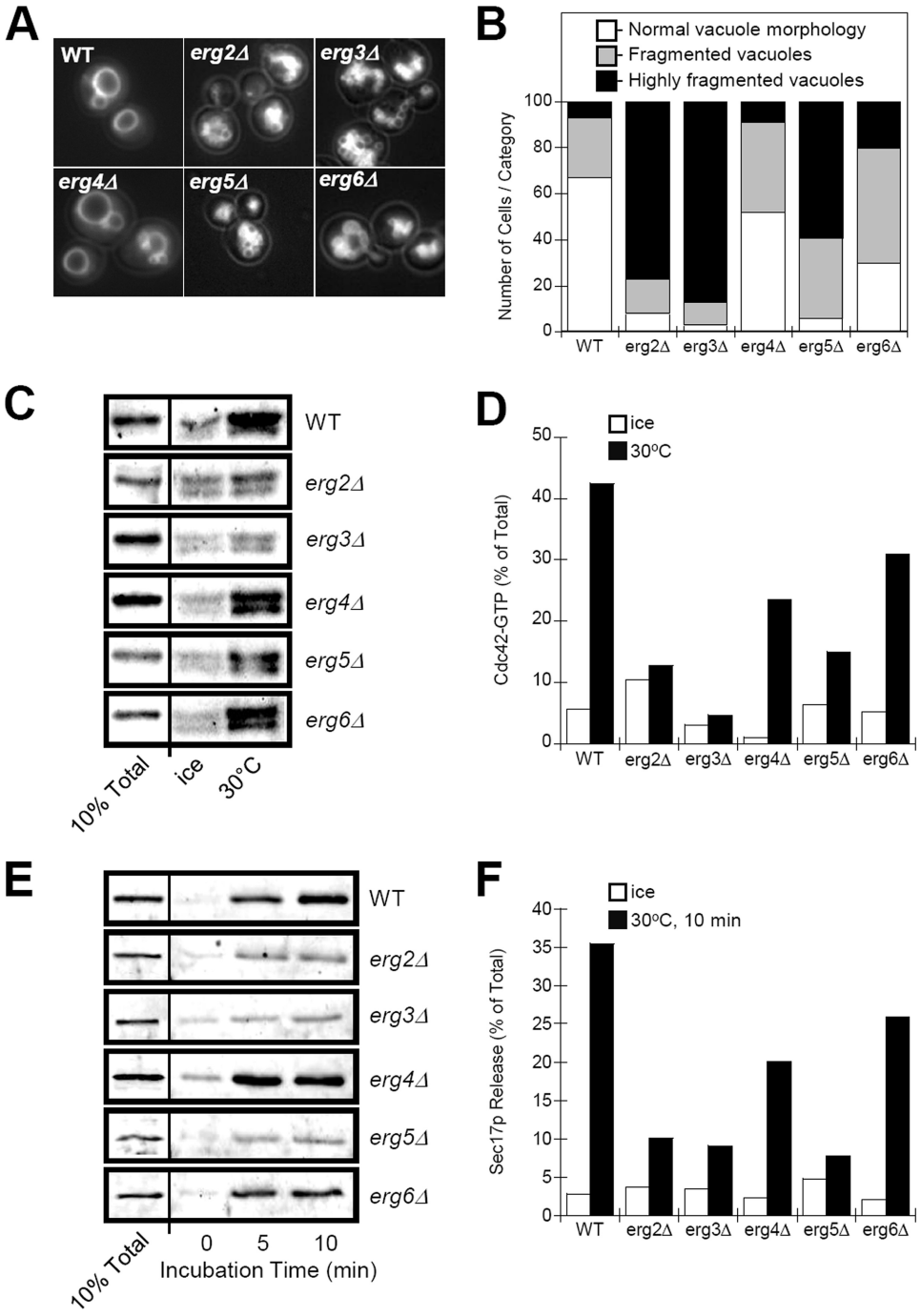


FIGURE 7. **Effect of ergosterol synthesis mutants on vacuole morphology and Cdc42p activation.** *A*, normal vacuole morphology in BY4742 (WT) is compared with aberrant vacuole morphology of *ERG*-gene deletion strains. Vacuoles were stained by incubation with 3 $\mu$M FM4-64 for 1 h followed by a 5 h chase in dye-free medium. Panels are 20 $\mu$m $\times$ 20 $\mu$m. *B*, quantification of vacuole fragmentation of *ERG*-gene deletion strains as described in the legend to Fig. 3. *C*, assay for Cdc42p activation on vacuoles isolated from *ERG*-gene deletion strains. Vacuoles, isolated from BY4742 (WT) or *ERG*-deletions strains as indicated, were incubated in F.R.B., ATPreg, cytosol, and 40 $\mu$M GTP$\gamma$S for 30 min at 30 °C or on ice. Levels of activated Cdc42p were determined by association with immobilized GST-CBD probe. *D*, quantification of Cdc42p activation as shown in *panel C*. *E*, assay for Sec17p released from vacuoles isolated from *ERG*-gene deletion strains. *F*, quantification of Sec17p release as shown in *panel E*. *10% Total* refers to load controls for Cdc42p (*C*) and Sec17p (*E*).

uole fragmentation in certain *ERG* gene-deletion strains (Fig. 7*A*) and reduced fusion competency *in vitro*.[3] Deletion of *ERG* genes also affected vacuolar Cdc42p activation. We found significant correlation between the levels of vacuole fragmentation in *ERG* gene-deletion strains and Cdc42p activation. *erg2*, *erg3*, and *erg5* strains showed the highest levels of vacuole fragmentation (Fig. 7*B*) and greatly reduced Cdc42p activation (Fig. 7, *C* and *D*, compare *ice* to *30* °C). The *erg4* and *erg6* strains showed intermediate levels of vacuole fragmentation and a partial reduction in Cdc42p activation. Interestingly, priming-dependent Sec17p release was also defective in *erg2*, *erg3*, and *erg5* strains (Fig. 7, *E* and *F*). From these data we conclude that Cdc42p activation is sterol-dependent and occurs as one of the first steps of vacuole priming for fusion.

## DISCUSSION

Rho proteins govern the initiation of many spatially defined signaling processes, and hence it is not surprising to find them localized to many intracellular sites (21). We have previously shown that two Rho GTPases, Cdc42p, and Rho1p, are enriched on the vacuole membrane, where they participate in the regulation of membrane fusion (22). Cdc42p controls vacuole-associated actin remodeling, whereas the role of Rho1p is undefined. Here we report our examination of the Cdc42p activation cycle and its affect on vacuole fusion. We prepared constitutively active and dominant-negative mutants of Cdc42p with inducible expression from the *GAL1* promoter. Mutant allele expression in the absence of functional Cdc42p (*i.e.* expression in *cdc42-1* at 37 °C) or high levels of overexpression with 2% galactose was toxic to cells (not shown), which is similar to previous results (15). Therefore, we used growth conditions that allowed for minimal effects on cell viability (doubling time increase was not more than 20% in all strains) yet still obtained significant overexpression of Cdc42p (Fig. 1).

Interestingly, mutations that disrupted GTP binding or GTP hydrolysis caused similar phenotypes including a large increase in the number of small vacuolar structures (*i.e.* vacuole frag-

[3] Y. M. te Welscher, L. Jones, M. R. van Leeuwen, J. Dijksterhuis, B. de Kruijff, G. Eitzen, and E. Breukink, submitted manuscript.

mentation). Therefore, contrary to the belief that the activated state is the primary requirement to initiate signaling, we found that Cdc42p cycling through active and inactive states was required for its activity. This explains the effect that we and others have observed that expression of either constitutively active or dominant-negative Rho proteins can lead to similar phenotypes (23, 24). Several other reports also support the need for cycles of GTP loading and hydrolysis for full functionality (25–27). Overexpression of wild-type Cdc42p also caused an increase in vacuole fragmentation. This is likely due to prolonged GDP or GTP-bound states because cycling factors such as GEFs and GAPs may be limiting at high levels of Cdc42p. This also implicates an extended need for upstream regulators of Cdc42p (*i.e.* GEFs and GAPs; see Ref. 28) to participate in downstream signaling processes.

Although overexpression of all *CDC42* alleles resulted in vacuole fragmentation, this phenotype was not maintained during cell stress. Brief exposure to hypotonic stress can be used to stimulate rapid vacuole fusion (12), which occurred in almost all strains (with exceptions discussed below). We explain this as the difference in steady-state *versus* stimulated morphology. At steady-state, an accumulated morphological defect of fragmented vacuoles is due to the presence of high levels of Cdc42p that does not undergoing rapid cycling. This accumulated defect was bypassed by exposure to new fusion stimuli (hypotonic shock), which triggered rapid vacuole fusion. Therefore, an initial round of fusion only requires activated Cdc42p since fusion was blocked by non-activatable Cdc42p-T17N (Fig. 2, compare *j* to *n*). Likewise, *in vitro* vacuole fusion, which occurs primarily as a single round of fusion (29), was inhibited by Cdc42p-T17N, but kinetically enhanced by constitutively active Cdc42p-G12V (Fig. 4). However, when multiple rounds of vacuole fusion were examined using sequential hypertonic-hypotonic stimuli, expression of both constitutively active and dominant-negative alleles of Cdc42p inhibit fusion (Fig. 2, *Hypotonic 2*). These data strongly suggest that cycles of Cdc42p activation are required for multiple rounds of fusion.

We have previously shown that the Rho guanine dissociation inhibitor, Rdi1p, blocks the fusion of purified vacuoles (22). Rdi1p should block the activation of Cdc42p, however, previous experiments did not directly examine the activation processes. We have now adapted a method to detect yeast Cdc42p activation in *in vitro* reactions (10). We rigorously tested this assay using recombinant Cdc42p proteins and chemical nucleotide exchange experiments and found that only GTP-bound Cdc42p interacted with the activation probe (Fig. 5). Activation probes also verified the specificity of the Cdc42p mutant alleles since nucleotide-locking amino acid modification behaved as expected; no interaction with the dominant-negative mutant and enhanced interaction with the constitutively-active mutant (Fig. 5*B*). This assay was able to detect significant activation of Cdc42p during vacuole fusion reaction. Incubation of membranes in the presence of Rdi1p blocked Cdc42p activation as did incubation on ice (Fig. 6*C*). Hence, the Cdc42p activation mechanism is clearly driven during incubation for membrane fusion.

Kinetic analysis showed that Cdc42p was rapidly activated when membranes were incubated in conditions that stimulated fusion. This is in accord with the early kinetic stimulation of fusion when constitutively active Cdc42p-G12V is expressed (Figs. 6*B* and 4*B*). We have recently shown that Cdc42p regulates vacuole-associated actin remodeling, which is required for the final stages of membrane fusion (4, 5). Thus, the regulation of Cdc42p activation at an earlier stage (*i.e.* priming) provides the correct temporal initiation of signaling to actin remodeling, but exactly how this is coupled to the membrane fusion mechanism is unknown. Our data support the theory that F-actin formation facilitates membrane fusion since the coupling of these mechanisms during exocytosis has been shown in many systems. Clear examples of actin regulated fusion include GLUT4 and insulin vesicle exocytosis in adipose and islet cells (30, 31), chromaffin granules in neuroendocrine cells (7, 32) and primary granules in neutrophils (33). Therefore, Cdc42p activation provides an additional layer of regulation for membrane fusion through actin remodeling which may be common to many secretory processes (34).

Several lines of evidence clearly show a requirement for Cdc42p activation for membrane fusion; however, less clear is whether the Cdc42p activation and membrane fusion mechanisms are intimately linked. The time course of Cdc42p-GTP appearance suggested that Cdc42p activation is linked to the priming subreaction of fusion, however, typical priming inhibitors, such as Sec17p and Sec18p ligands, did not affect Cdc42p activation (Fig. 6). Other membrane fusion factors, such as Rabs and SNAREs, function at membrane docking which occurs after priming (17). Priming is dependent on ergosterol (19), and our examination clearly showed a dysfunction in Cdc42p activation in specific mutants of the ergosterol biosynthetic pathway (Fig. 7). Interestingly, mutants that showed the highest levels of vacuole fragmentation were most affected in Cdc42p activation. The analysis of Sec17p release in these strains also showed clear linkage to vacuole fragmentation levels. These data support the existence of a mechanistic connection between ergosterol-depenent Cdc42p activation and Sec17p/Sec18p-dependent membrane priming for fusion.

*Acknowledgment—We thank Dr. William Wickner for providing Sec17p and Sec18p antibodies.*

## REFERENCES

1. Johnson, D. I. (1999) *Microbiol. Mol. Biol. Rev.* **63,** 54–105
2. Hall, A. (2005) *Biochem. Soc. Trans.* **33,** 891–895
3. Ridley, A. J. (2006) *Trends Cell Biol.* **16,** 522–529
4. Eitzen, G., Wang, L., Thorngren, N., and Wickner, W. (2002) *J. Cell Biol.* **158,** 669–679
5. Isgandarova, S., Jones, L., Forsberg, D., Loncar, A., Dawson, J., Tedrick, K., and Eitzen, G. (2007) *J. Biol. Chem.* **282,** 30466–30475
6. Gasman, S., Chasserot-Golaz, S., Malacombe, M., Way, M., and Bader, M. F. (2004) *Mol. Biol. Cell* **15,** 520–531
7. Tedrick, K., Trischuk, T., Lehner, R., and Eitzen, G. (2004) *Mol. Biol. Cell* **15,** 4609–4621
8. Pruyne, D., and Bretscher, A. (2000) *J. Cell Sci.* **113,** 365–375
9. Jansen, G., Wu, C., Schade, B., Thomas, D. Y., and Whiteway, M. (2005) *Gene* **344,** 43–51
10. Benard, V., Bohl, B. P., and Bokoch, G. M. (1999) *J. Biol. Chem.* **274,** 13198–13204
11. Haas, A. (1995) *Methods Cell Sci.* **17,** 283–294
12. Wang, Y. X., Kauffman, E. J., Duex, J. E., and Weisman, L. S. (2001) *J. Biol.*

*Chem.* **276,** 35133–35140
13. LaGrassa, T. J., and Ungermann, C. (2005) *J. Cell Biol.* **168,** 401–414
14. Drees, B. L., Sundin, B., Brazeau, E., Caviston, J. P., Chen, G. C., Guo, W., Kozminski, K. G., Lau, M. W., Moskow, J. J., Tong, A., Schenkman, L. R., McKenzie, A., 3rd, Brennwald, P., Longtine, M., Bi, E., Chan, C., Novick, P., Boone, C., Pringle, J. R., Davis, T. N., Fields, S., and Drubin, D. G. (2001) *J. Cell Biol.* **154,** 549–571
15. Davis, C. R., Richman, T. J., Deliduka, S. B., Blaisdell, J. O., Collins, C. C., and Johnson, D. I. (1998) *J. Biol. Chem.* **273,** 849–858
16. Seeley, E. S., Kato, M., Margolis, N., Wickner, W., and Eitzen, G. (2002) *Mol. Biol. Cell* **13,** 782–794
17. Wickner, W. (2002) *EMBO J.* **21,** 1241–1247
18. Peter, M., Neiman, A. M., Park, H.O., van Lohuizen, M., and Herskowitz, I. (1996) *EMBO J.* **15,** 7046–7059
19. Kato, M., and Wickner, W. (2001) *EMBO J.* **20,** 4035–4040
20. Fratti, R. A., Jun, Y., Merz, A. J., Margolis, N., and Wickner, W. (2004) *J. Cell Biol.* **167,** 1087–1098
21. Michaelson, D., Silletti, J., Murphy, G., D'Eustachio, P., Rush, M., and Philips, M. R. (2001) *J. Cell Biol.* **152,** 111–126
22. Eitzen, G., Thorngren, N., and Wickner, W. (2001) *EMBO J.* **20,** 5650–5656
23. Moorman, J. P., Luu, D., Wickham, J., Bobak, D. A., and Hahn, C. S. (1999) *Oncogene* **18,** 47–57
24. Vanni, C., Ottaviano, C., Guo, F., Puppo, M., Varesio, L., Zheng, Y., and Eva, A. (2005) *Cell Cycle* **4,** 1675–1682
25. Gladfelter, A. S., Bose, I., Zyla, T. R., Bardes, E. S., and Lew, D. J. (2002) *J. Cell Biol.* **156,** 315–326
26. de Toledo, M., Senic-Matuglia, F., Salamero, J., Uze, G., Comunale, F., Fort, P., and Blangy, A. (2003) *Mol. Biol. Cell* **14,** 4846–4856
27. Fidyk, N., Wang, J. B., and Cerione, R. A. (2006) *Biochemistry* **45,** 7750–7762
28. Gulli, M. P., and Peter, M. (2001) *Genes Dev.* **15,** 365–379
29. Merz, A. J., and Wickner, W. T. (2004) *Proc. Natl. Acad. Sci. U.S.A.* **101,** 11548–11553
30. Lopez, J. A., Burchfield, J. G., Blair, D. H., Mele, K., Ng, Y., Vallotton, P., James, D. E., and Hughes, W. E. (2009) *Mol. Biol. Cell* **20,** 3918–3929
31. Nemoto, T., Kojima, T., Oshima, A., Bito, H., and Kasai, H. (2004) *J. Biol. Chem.* **279,** 37544–37550
32. Malacombe, M., Ceridono, M., Calco, V., Chasserot-Golaz, S., McPherson, P. S., Bader, M. F., and Gasman S. (2006) *EMBO J.* **25,** 3494–3503
33. Mitchell, T., Lo, A., Logan, M. R., Lacy, P., and Eitzen G. (2008) *Am. J. Physiol. Cell Physiol.* **295,** C1354–C1365
34. Wu, H., Rossi, G., and Brennwald, P. (2008) *Trends Cell Biol.* **18,** 397–404